Chaos, Solitons & Fractals 56 (2013) 194–201

Contents lists available at ScienceDirect

Chaos, Solitons & Fractals

Nonlinear Science, and Nonequilibrium and Complex Phenomena

journal homepage: www.elsevier.com/locate/chaos

Peloton phase oscillations

Hugh Trenchard

805 647 Michigan Street, Victoria V8V 1S9, Canada

ARTICLE INFO

Article history:
Available online 6 September 2013

ABSTRACT

A peloton may be defined as two or more cyclists riding in sufficiently close proximity to be located either in one of two basic positions: (1) behind cyclists in zones of reduced air pressure, referred to as 'drafting', or (2) in non-drafting positions where air pressure is highest. Cyclists in drafting zones expend less energy than in front positions. Qualitative observations of pelotons indicate oscillations between two primary phases. The first is a high density, low speed/power output phase. The second is a synchronized, low density, high speed or power output phase. Pelotons are observed to oscillate between phases, and mixed phases occur. Principles determining the first phase are coupling due to the energy savings of drafting, collision avoidance, and continuous passing. Principles determining the synchronized phase are similar, except that minimal passing is observed in this phase as cyclists approach maximum sustainable outputs. Phases self-organize as cyclists proceed through output thresholds, while strategic and tactical considerations are secondary. A computational simulation with an algorithm combining a coupling ratio, passing time, and constraints on angles of alignment, separation and cohesion (flocking rules), demonstrates phase oscillations.

1. Introduction

The Tour de France is perhaps the best known mass-start bicycle race. It is a race among ~200 riders who compete for top individual and team placing and cover distances up to 220 km over 23 days (www.letour.fr, 2012). Mass-start bicycle races are also held on oval tracks called velodromes. Standard track lengths are 250 m or 333 m. Track races consist of multiple laps, and may be between 3 and 40 km in distance, composed of perhaps 15–40 riders. Mountain bike and cyclo-cross events are also mass-start races, but these are not discussed here, since they usually involve narrow courses on which riders are forced to ride single-file and do not generate the kinds of dynamics explored here.

On one hand, a peloton may be characterized as the collection of cyclists (or "riders") in a given mass-start competition, each of whom employ tactics and strategy for the top positions at the finish line. In this view, collective peloton behaviors result from the activation of deliberate and calculated competitive objectives of the riders, and collective peloton behaviors are therefore top-down in nature.

An analysis of peloton dynamics on the basis of top-down influences may well enable a sound understanding of cycling as a sport. However, a fuller appreciation of the richness of peloton dynamics is achieved by a conception of a peloton as a complex dynamical system. Under a complex systems approach, certain collective dynamics are self-organized and emerge from physical principles that drive cyclists' local, or nearest neighbor, interactions. These collective behaviors and patterns emerge independently of the riders' deliberate competitive actions, and cannot be predicted by the behaviors of individual cyclists riding in isolation from the group.

Pelotons may also be considered to be a special case of the more general category of flocking systems. Pelotons entail aspects of flocking dynamics because, like flocks, they involve principles of collision avoidance, velocity matching, and some elements of "flock centering", the attempt to stay close to nearby neighbors. Craig Reynolds [1] simulated these principles for bird flocks with rules to

E-mail address: htrenchard@shaw.ca

0960-0779/$ - see front matter © 2013 Elsevier Ltd. All rights reserved.
http://dx.doi.org/10.1016/j.chaos.2013.08.004

determine bird alignment, separation and coherence. For developments and variations of flocking models, see for example [2–5].

In pelotons, cyclists are heterogeneous biological oscillators with different maximum fitness capacities, referred to here as maximal sustainable outputs ("MSO"). This determines cyclists' capacity to keep pace with the group; it also determines cyclists capacity to pass those ahead, which falls in inverse proportion to increasing fraction of MSO.

For any given competitive level (i.e. racing category), the variance in cyclists' fitness level is generally sufficiently narrow so that energy savings by drafting more than equalizes these differences. Unless drafting is negligible, such as up steep hills, as shown in Fig. 5, heterogenous differences in fitness have small effects on peloton dynamics. The equalizing effect of drafting is the basis for cyclists' race strategy and tactics, but it is also the fundamental driver of the peloton as a self-organizing system.

The energy savings principle, fundamental to peloton dynamics, is an essential distinction between the peloton model developed here and existing flocking models, which generally do not account for the effects of optimal positioning due to energy savings. Energy savings benefits of flying in certain optimal positions has been well demonstrated in two-dimensional, or v-formation flocks [6] and other biological formations [7–10], but considerable work remains to address this factor in terms of collective dynamics. The peloton model here predicts analogous peloton dynamics in conditions where fatigue is a significant factor during sustained biological locomotion and where optimal positions produce reductions in power output or energy expenditure.

2. Energy expenditure reduction by drafting

Drafting cyclists can sustain the same speed of non-drafting cyclists at lower average power output. Pelotons of up to 20 riders will travel faster than pelotons of lesser size, with a steep increase in speed, relative to smaller groups, from 1 to 5 riders, and a flattened increase in group speed between 5 and about 20 riders [11].

A cyclist's power requirement to overcome wind resistance is proportional to the cube of his or her velocity [12]. Power requirements when drafting a single rider is reduced by approximately 18% at 32 km/hr (19.9 mph), 27% at 40 km/h (24.9 mph), and by as much as 39% at 40 km/h in a group of eight riders [13]. Drafting benefit is negligible at speeds greater 16 km/h (9.9 mph) for two riders [14].

Based on the these energy savings values, a useful approximation is to describe the power output reduction when drafting as approximately 1% per mph behind a single rider, as shown in Fig. 1. For simplicity, this analysis applies this 1% per mph drafting magnitude. Here speeds here are shown in both English and metric values. Thus, at the elite level, speeds of 40 km/h (24.9 mph) to 50 km/h (31.1 mph) on flat topography are common. Pelotons of 100 or more riders are common.

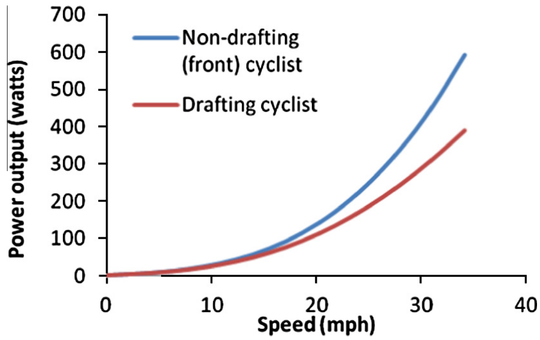

Fig. 1. Power requirements for cyclists in non-drafting position and in drafting position. Curve for non-drafting cyclist based on 75 kg (bicycle and rider); rolling friction coefficient 0.004 dimensionless; 0.00 gradient; air-density 1.226 kg/m^3; drag co-efficient of 0.5; frontal surface area of 0.05 m^2. Parameters from [20]. Curve for drafting cyclist based on savings of approximately 1% per mph (~1.6% per km/h).

In the simplified case of no lateral wind, optimal wheel spacing for drafting is directly behind riders ahead and about 0.5 m from the rear wheel of the front rider to the front wheel of the following rider [11]. Drafting benefit approaches zero at 3 m [11], while it is recognized that there may be some drafting benefit up to 10–12 m [15], or more [16].

Cyclists' power output is not determined only by speed; it may vary according to riders' position (drafting or non-drafting), their speeds being equal; also, speed falls in proportion to the slope of the road [14], while power output may remain constant. In this way, a weaker cyclist can maintain the speed of a stronger rider by drafting. But if power output is kept constant and the course gradient increases (uphill), speeds fall as does the drafting advantage, as shown in Fig. 5.

Conversely, speeds on descents may be high, but power output low. A literature search revealed no published research on cyclists' energy expenditure reductions due to drafting on descents. However, while proceeding down sufficiently steep descents, a front rider will reach terminal velocity at approximately 70 km/h (43.5 mph), the speed at which maximal output will result in negligible increases in speed [14]. So, at terminal velocity or faster, non-drafting riders will likely proceed without pedaling (no power output), just as the cyclists behind will do. In such a case the front-riding, non-drafting cyclists' power output is not significantly greater than that of a drafting rider. However, in such circumstances, following riders can "sling-shot" past front riders due to the combination of the low air-resistance of drafting and the accelerating effects of gravity.

On shallower descents in which front riders require high power output to increase speed (i.e. <terminal velocity), cyclists well know that drafting reduces power output by magnitudes approaching 100% relative to a front rider generating near maximal power output. This substantial imbalance in power output between front and following riders on shallow descents often results in a rotational dynamic where following riders continuously pass those in front. This process, described here as a convection dynamic, is also observed at low-to-mid-ranges of collective power output on any given race course gradient.

3. Cyclists' physiological parameters

Human physiological or athletic capacities may be generalized to encompass three basic categories of MSO. More precisely, MSO refers to metabolic power production sustainable for specific times to exhaustion as a fraction of $V02_{max}$ or maximum volume of oxygen consumed in liters/min [11].

As a guide, consistent with the definitions above, a sprint of maximal anaerobic output (90% anaerobic) is sustained for less than ten seconds, while a sub-maximal effort (50/50 anaerobic/aerobic requirement) is sustainable for approximately two minutes; an aerobic output (99% aerobic) may be sustained for hours [17]. Sprint efforts for males may be carried out at peak power outputs of approximately 1100–1200 W [18], while sub-maximal efforts among elite male cyclists may be carried out approximately between 350 and 525 W [19], and aerobic efforts occur at ranges below 350 W.

4. Complex dynamics of pelotons

At its foundation, peloton dynamics are largely attributable to the physical requirement that cyclists avoid collisions, the coupling effects of drafting, and the capacity for cyclists to pass others. By exploiting the reduced power output requirement of drafting, a drafting cyclist's power output is coupled to the rider ahead, and by alternating between non-drafting and drafting positions, cyclists' outputs are mutually coupled. Under a process of continuous collective positional change, all the riders in a peloton are globally coupled. Drafting is in turn a major determinant of cyclists' capacity to pass each other, in addition to their inherent physiological capacity to accelerate.

These coupling effects are fundamental to the emergence of complex dynamics and observable phase changes in pelotons. As power-output and speeds change throughout the course of a mass-start race, peloton density oscillates, as shown in Figs. 2, 3 and 7. In Fig. 2, data was obtained from a "points race" on a velodrome, a 30 km race in which points are awarded to the top five riders across the line every five laps; highest accumulated points at the finish wins. By contrast, the 75 lap (900 m/lap) criterium race shown in Fig. 7, is a race in which the top places are awarded strictly by final finishing order.

The threshold at which cyclists de-couple may be described by Eq. (1). It encompasses a simplified instance of cyclists' coupling dynamics where the difference between the MSOs of a stronger rider in a non-drafting position rel-

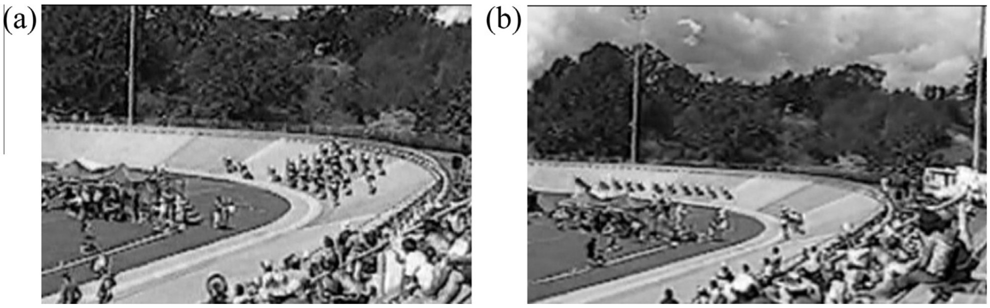

Fig. 2. Oscillating peloton density: (a) high density; (b) stretched, or single-file, pace-line formation, at low density. In this velodrome "points-race", peloton speeds are highest in the stretched condition, while speeds are lowest in high density formations. Note that speeds during this event did not drop below 37 km/h (23 mph).

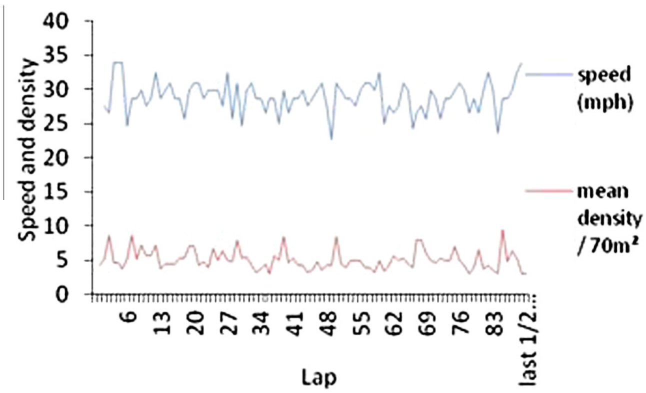

Fig. 3. Peloton speed and density during 30 km (18.6 mile) points race on velodrome. Upper curve represents speed of first rider across the line (mph) over 90 laps (half lap plus 90 laps), assumed to represent the average speed of the peloton. Lower curve represents peloton density. Peaks of highest speeds correspond to lowest density points, and vice versa.

ative to a weaker, drafting rider, is equalized by the drafting benefit. This is referred to here as the Peloton Divergence Ratio (PDR) [21], given by:

$$\mathrm{PDR}\left[\frac{(W_{front} - W_{draft})}{W_{front}}\right] \Big/ \left(\frac{D}{100}\right) \tag{1}$$

where W_{front} is the MSO (watts) of front (non-drafting) cyclist A at any given moment; W_{draft} is the MSO of drafting cyclist B at any given moment (assuming $W_{front} > W_{draft}$) ignoring negligible differences in equipment, body mass and volume, and assuming approximately similar on-bike body positions; $D/100$ is the percent energy savings (correlating to reduced power output) due to drafting at the velocity traveled. This is called a divergence ratio because it reveals the critical power output threshold at which coupled riders de-couple. More succinctly, PDR shows the proportion of strength a weaker rider, B, must be to a stronger one, A, before B cannot keep up to A while drafting.

However, non-drafting riders will not always travel at their MSO, nor is the non-drafting rider necessarily stronger than the following. So, it is useful to model coupling situations in which the front rider is not traveling at MSO and is not assumed to be stronger than the following rider. At the same time, the following rider may also not be traveling at MSO, but nonetheless matches the speed of the front rider with reduced energy requirements due to drafting, whether by necessity or not. In these circumstances:

$$\mathrm{PCR} = \frac{\left[P_{qfront} - \left(P_{qfront} * \left(\frac{D}{100}\right)\right)\right]}{P_{maxdraft}} \tag{2}$$

where PCR is the Peloton Convergence Ratio;

P_{qfront} is the power output of the front rider at the given speed and equals the power output required by the following, drafting rider, to maintain the speed set by the front rider if the following rider were not drafting (hence "required output"); $P_{maxdraft}$ is the MSO of the following rider.

PCR may be described simply as a ratio of the following rider's required output for the given speed, minus D, over her maximum output, where the speed and drafting component are determined by the front rider. As for PDR, differences in equipment, body frontal surface area or body position, are ignored and it is assumed that each cyclist requires approximately the same power to proceed in non-drafting or drafting positions at any given speed.

The key distinction between PDR and PCR is that for PCR, the required output of the following rider is established by the front, non-drafting, rider, but the front rider's MSO need not be known or assumed. The front rider cannot, of course, exceed her own MSO, but may be riding at any output less than MSO. However, the required output, as set by the non-drafting front rider, may exceed the MSO of the following rider. The *actual* output of the following rider at the speed set by the front rider, is that which has been reduced by drafting benefit D. Thus when PCR < 1, a following rider maintains the required output for the given speed set by the front rider, and when PCR > 1, the two riders will de-couple, as shown in Fig. 4.

Generally, divergences between riders occur when PCR exceeds 1. These divergences may be temporary, but divergences increase in frequency and duration during periods of low peloton density; i.e. when the peloton stretches and all riders approach PCR 1. When PCR < 1 for all riders, cyclists remain coupled.

As cyclists' power output parameter changes, qualitative observations of pelotons indicate that peloton dynamics encompass four major phase regimes. These phases represent the predicted behavior that may be observed in a computational peloton simulation. Phases are qualitatively described by the following:

I. Relaxed: Cyclists proceed at low power outputs and low PCR; because optimal drafting is not required at low-outputs, the peloton is of sub-maximal density. At the start of a competitive event, this is a temporary state as cyclists increase outputs to racing speeds. However, equivalent low-outputs are achieved at high speeds on descents when cyclists temporarily cease pedaling.

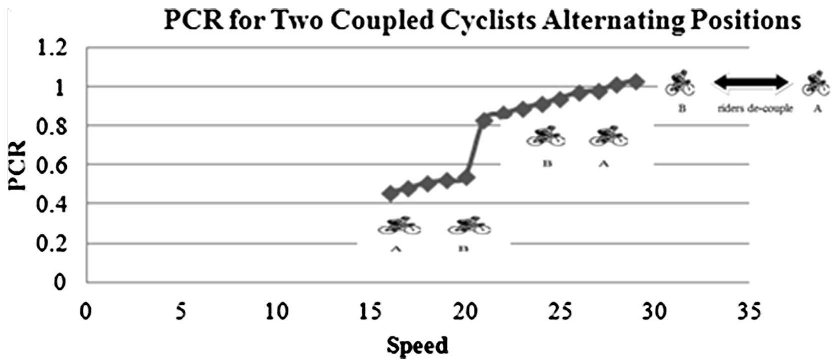

Fig. 4. Applying approximate energy savings of 1% per mph, illustration shows two coupled cyclists where a weaker rider begins in front and proceeds to maximum speed and output, and who then changes position with a stronger rider, allowing the weaker rider to draft and to continue increasing speed beyond her maximum speed capable without drafting. Thus over speeds 16–20 mph, weaker rider B is in front while stronger rider A is drafting. When B reaches maximum output at 20 mph, riders change positions so A is in front and B is drafting. PCR is in lower range when stronger rider drafts, and curve jumps to higher range when they switch positions. When D no longer offsets the difference between front (stronger) rider's output and the following (weaker) rider's maximum, PCR > 1 and riders de-couple.

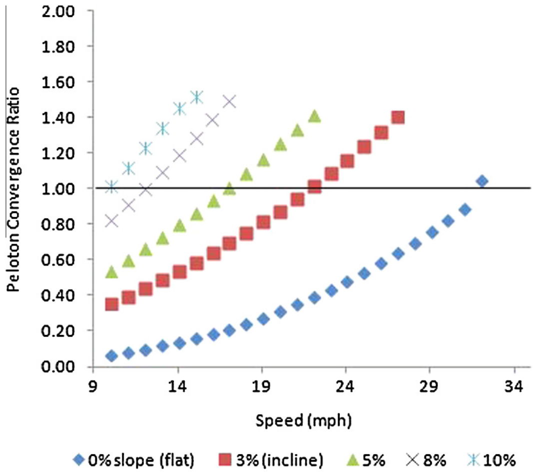

Fig. 5. PCR as a function of cyclist speed, and course gradient (hill) over five incline grades. For the speeds shown, by taking advantage of the energy savings of drafting a following cyclist with a hypothetical maximum sustainable output of 349w, based on the range of outputs reported in [19], on a flat, windless course, can maintain the speed of a rider ahead (who may or may not also be drafting behind other riders) up to about 32 mph (51.5 km/h). Above this speed, a stronger rider capable of the output required to attain the speeds shown, will ride away from the weaker cyclist. This is shown by the point at which PCR > 1. However, at a 3% grade, the same drafting cyclist will be able to maintain the speed of a rider ahead up to about 22 mph (35.4 km/h). At grades of 10% or more, a cyclist in front, even marginally capable of greater power output than the drafting cyclist, will pull ahead. Required power outputs for the speeds and grades shown for a cyclist capable of 349w were obtained by using the computation application in [20], applying the same group of parameters as shown in Fig. 1. Windless conditions are assumed.

II. Convection (high density): This phase emerges within a mid-region of PCR < 1. It is characterized by riders advancing up peloton peripheries as riders in central positions, where density is too high to allow effective passing in central regions, shift their positions effectively backward. Peloton density approaches maximum. Passing occurs in continuous rotation, and by analogy may be viewed as forming a convection dynamic whereby groups of "warming" cyclists advance up the peripheries, and "cooling" cyclists effectively shift backward along central trajectories within the peloton, as shown in Fig. 6, and indicated in Figs. 2, 7 and 8(a).

III. Synchronized (low density): As riders approach MSO, PCR approaches 1, and cyclists' speeds are sufficiently high so as to reach a critical threshold when riders self-organize into a single-file paceline, where cyclists ride one immediately behind another, as shown in Figs. 2,7,8 (b).

IV. Disintegrated: Riders de-couple and separate. PCR > 1 in conditions of low drafting benefit, such as on hills as shown in Fig. 5; or when riders' efforts are near sprint MSO during an intermediate attack (a near sprint effort to escape from the peloton), or during a finishing sprint when riders must pull out of drafting zones into non-drafting positions in order to attempt to cross the finish line first, as shown in Figs. 7 and 8(d).

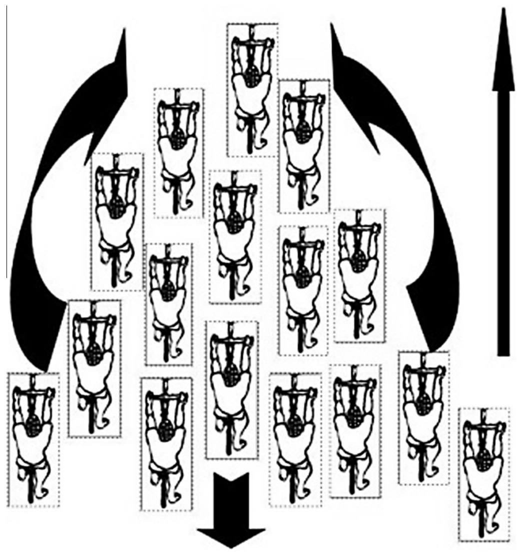

Fig. 6. Peloton convection. Long straight arrow indicates direction of peloton. Curved arrows indicate general rotation: riders pass up peloton peripheries as central areas within the peloton are too dense for rapid passing. Notched arrow indicates effective direction of riders in the middle of the peloton as they are passed by riders moving up peripheries.

5. Simulation algorithm, results and observations

The two main components of the peloton algorithm applied here are: (1) a passing rule; (2) the application of flocking rules, first simulated by Reynolds [1].

The passing algorithm applies the following general equation, which is a modification of the basic equation $t = d/v$:

$$Pt = (dfn^2/m)/\left[p - (p^* PCR^1)\right] \tag{3}$$

where pt is passing time; dfn is the distance to the farthest neighbor to a given maximum; m is the square of the maximum dfn; p is the current power output, initialized as a changing random value within a narrow range.

For this model, PCR^1 is a variable ratio, adjusted manually. It applies the values produced by PCR (Eq. (2)). As a fractional value, no specific power output values need be incorporated, since PCR^1, like PCR, encompasses all the power-output relationships between drafting and non-drafting cyclists.

Note that successful simulations were run using only PCR in the denominator of this equation. However for the purposes of the present simulation, the term $p-(p * PCR^1)$ reflects a power output value equivalent to velocity (adjusted according to race course gradient, as discussed); therefore the equation is a modified $t = d/v$ equation that describes a passing dynamic where the time required for cyclists to pass those ahead increases as PCR increases. Note the Netlogo simulation algorithm incorporating this equation is set for absolute values and operates only if values are >0.

For the tests run here, dfn value was eight. This indicates that if there eight or more cyclists ahead, the

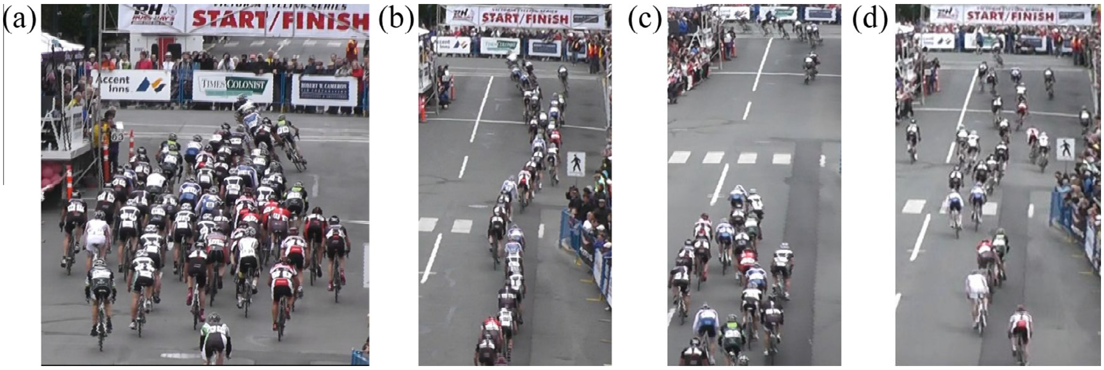

Fig. 7. Four states of peloton density: (a) highest density, length, and comparatively low collective speed; (b) low density, high peloton length and high synchronized speed; (c) peloton split (note group at top of image), high peloton length; (d) group is disintegrated at the race finish as riders de-couple, traveling at varied speeds.

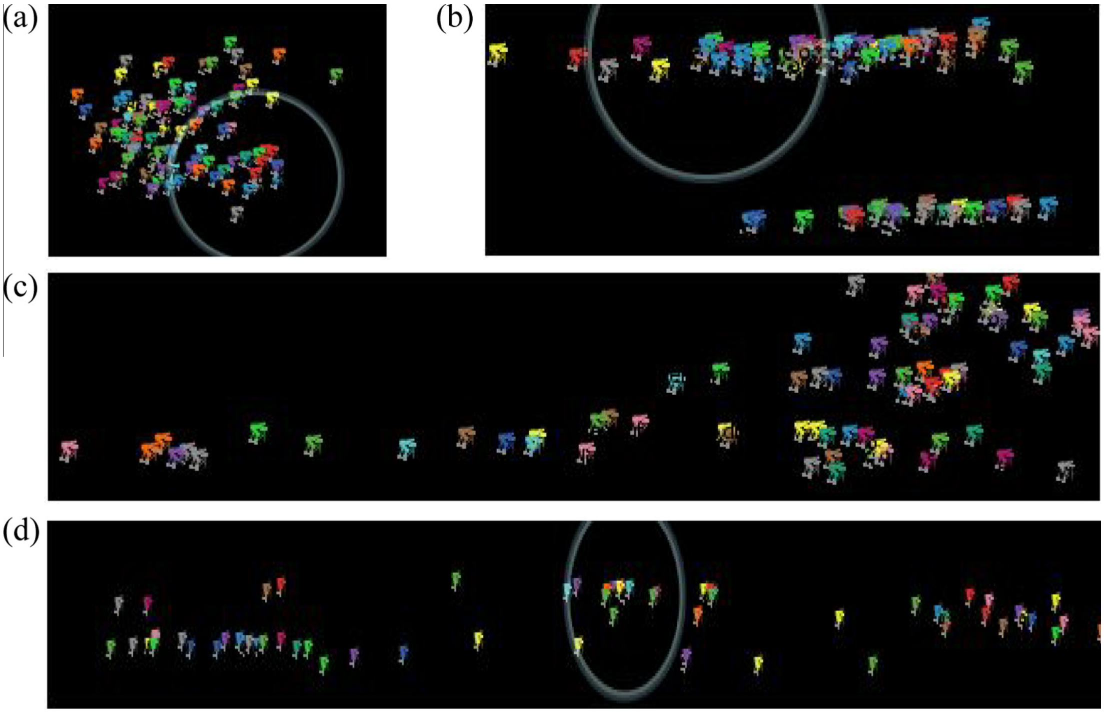

Fig. 8. (a) typical low density state (PCR = 0.50); (b) typical stretched state, with two-group split (PCR = 0.66); (c) typical mixed state of stretching and low density (PCR = 0.58); (d) typical disintegration (PCR = 0.95).

equation applies the maximum (value 8). However, if there are any number less than eight riders ahead, then this *dfn* is correspondingly smaller, but never less than one. An internal Netlogo algorithm counts a minimum value of 1 for this operation [22]. Here the value 8 was selected heuristically and reflects the approximated situation in which a rider may pass up to eight riders at a time, before fatiguing and decelerating. The term dfn^2/m is a fraction of the passing capacity to the maximum passing distance.

The second major component of the peloton algorithm here adapts three flocking rules, first simulated by Reynolds [1]: alignment, cohesion, and separation (the "ACS" rules). The ACS rules were incorporated into a Netlogo model by Uri Wilenksi [23]. Here attempts were made to develop a peloton model that did not incorporate the ACS rules, and while some limited success was achieved, collective motion was ultimately unrealistic and it is argued here that the ACS rules, or some equivalence of their mean-heading principle, are necessary elements of a peloton model.

Each of the elements of ACS facilitate the broader flocking principles of collision avoidance, velocity matching, and flock centering [1]. Here each of the three ACS rules were set initially to narrow angles, and all three ACS parameters were set at >89°, and approached 90° (which in Netlogo is directly facing right), and varies in correspondence to PCR. In this way, simulated cyclists travel within a narrow range of angles to the right of the universe and according to the ACS.

It is emphasized that the parameters *dfn* and its corresponding *m*, as well as the initial narrow random *p* values, and ACS angle parameters, may all be adjusted to fine-tune peloton phase regimes, but the basic algorithm containing a passing distance parameter over a power output or speed parameter successfully models the general peloton behavior and phases. Further, while variations of the equation and algorithm here may prove to more accurately model peloton dynamics, the results here suggest that a successful model necessarily includes a passing rule that incorporates decreasing passing capacity as power output increases.

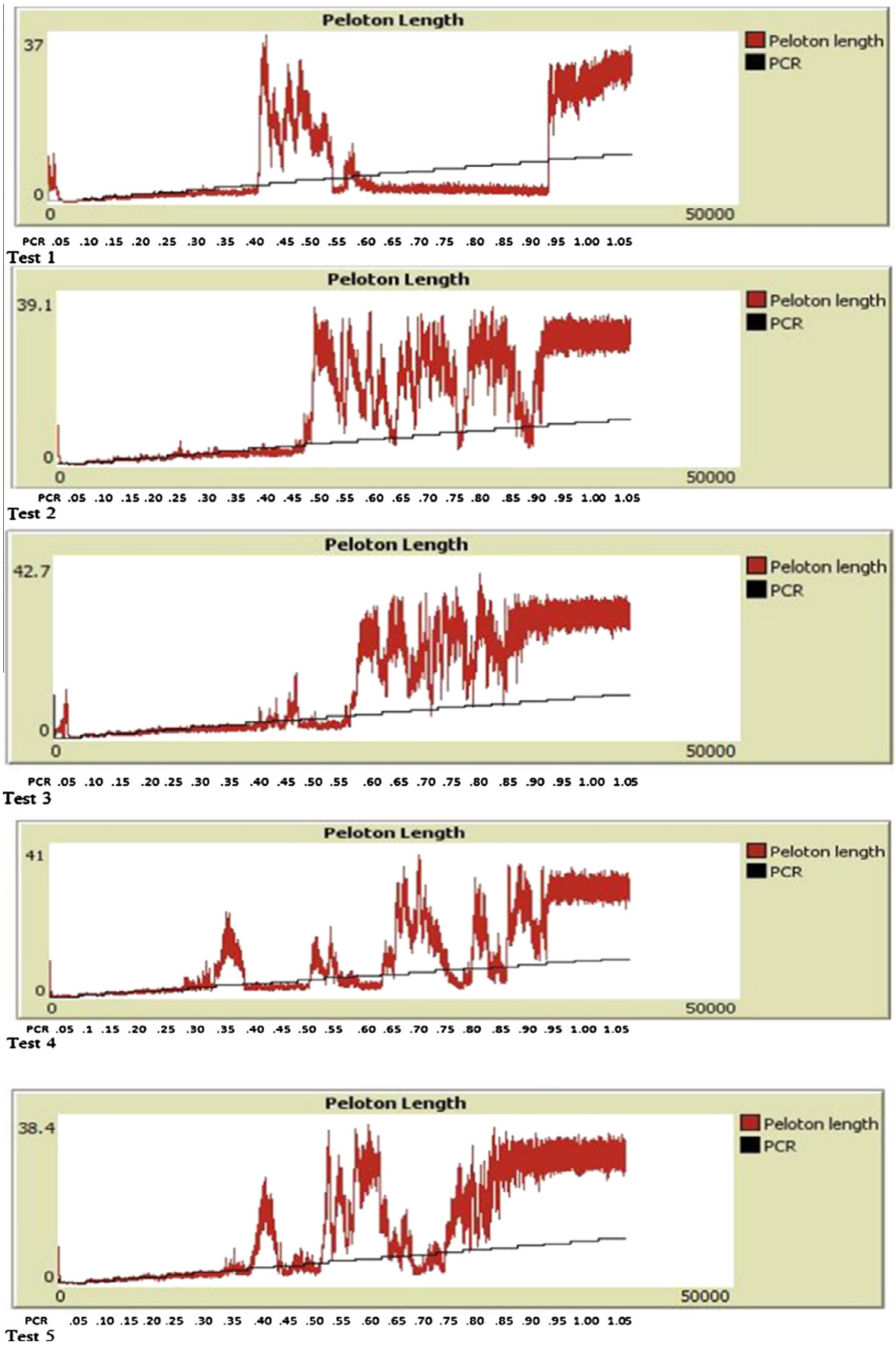

Fig. 9. Simulation results indicating a stable high density regime to ~PCR 0.35, a complex phase regime of oscillating densities between ~PCR 0.35 and ~PCR 0.80, and a stable low density, disintegrated, regime above ~PCR 0.85. In Test 1, note the long period of high density through increasing PCR before the rapid disintegration at PCR 0.95.

A Netlogo simulation that incorporates this general equation, demonstrates oscillations in peloton phases. Five tests were conducted in which each simulation was run for 2000 iterations for each of PCR 0.05 through to PCR 1.05 at increasing intervals of 0.05, as shown in Fig. 9. A stable, high density regime exists between PCR 0.05 to approximately PCR 0.35–0.45, with a clear transition to lower density that is frequently indicated by a division in the peloton into two or more sub-groups, and a consequent large increase in overall peloton length. Here peloton length is measured by the mean maximum distance other cyclists are from each other.

The densities for PCR 0.5 to approximately 0.15 approach single-point densities, and have no correspondence in reality. However, realistic densities appear above these values, and a stable regime is indicated up to approximately PCR 0.35. From there to PCR $\sim$ 0.85 or 0.90, we see the complex regime exhibiting density oscillations. A stable disordered regime occurs at approximately PCR > 0.85, similar to that shown in Fig. 8(d).

6. Conclusion and directions for future work

Peloton phases emerge as a function of changing peloton density, and here oscillations between phases have been observed and simulated. Qualitative observations that phases are a function of cyclists' coupling due to drafting, their changing power outputs as fractions of maximum sustainable output and passing capacity, are supported computationally by a Netlogo simulation. The mid-region of simulated complex dynamics and oscillations in mid-ranges of PCR between a high density and comparatively low speed, and a synchronized low density and comparatively high speed, as shown in Fig. 9, corresponds to the density oscillations indicated in Figs. 2, 3 and 7.

The advantage of the model here is that it applies PCR as a power output relationship between non-drafting cyclists and drafting cyclists. This fractional power output value is independent of speed, while it also accounts for speed as the determinant of the drafting benefit. Further, by incorporating a passing dynamic where cyclists' time taken to pass others is a function of a given initial passing distance over power output values and adjusted according to PCR, realistic complex behaviors are simulated.

The results indicate that fundamental complex behaviors of pelotons are self-organized and independent of cyclists' individual and team strategies or tactics. While arguably the passing principle itself is a tactical action, the passing principle is nonetheless a rule of local interaction without a necessary connection to a cyclist's winning strategy. In this view, the passing principle is due largely to the relatively greater potential energy available for passing implied by the energy savings benefits of drafting.

Further empirical studies of actual pelotons are required to test the foundations of this model. Here the convection dynamic, while observed qualitatively in actual pelotons and in the Netlogo simulation here, may in future be quantified. In addition, further research may reveal the extent to which top-down strategy and cyclists' volitional decisions influence complex peloton dynamics. This in turn may have implications for other mixed top-down/bottom up systems, such as economical, political, governance, or other human-driven systems. The complex dynamics of pelotons and their density oscillations, self-organizing as they do from an energy savings principle and a consequent passing principle, may have analogs in many other non-human biological systems.

Acknowledgments

The author acknowledges posthumously the interest and support of Gottfried Mayer-Kress; the thoughts and input of Demian Seale, and Ashlin Richardson.

References

[1] Reynolds CW. Flocks, herds, and schools: a distributed behavioral model. In: Maureen C. Stone, editor. SIGGRAPH '87 computer graphics, vol. 21(4); July 1987. p. 25–34.
[2] Motsch S, Tadmor E. A new model for self organized dynamics and its flocking behavior. J Stat Phys 2011;144. 923-94.
[3] Cucker F, Smale S. Emergent behavior in flocks. IEEE Trans Autom Control May 2007;52(5):852.
[4] Agueh M, Illner R, Richardson A. Analysis and simulations of a refined flocking and swarming model of cucker-smale type. Kinetic Related Models (KRM) March 2011;4(1):1–16.
[5] Vicsek T, Zafeiras A. Collective motion. Phys Rep August 2012;517 (3–4):71–140.
[6] Weimerskirch H, Martin J, Clerquin Y, Alexandre P, Jiraskova S. Energy saving in flight formation. Nature 18 October 2001; 413:697–8.
[7] Fish FE. Kinematics of ducklings swimming in formation: consequences of position. J Exp Zool 1995;273:1–11.
[8] Gilbert C, Blanc S, Le Maho Y. Energy saving processes in huddling emperor penguins: from experiments to theory. J Exp Biol January 1 2008;211:1–8.
[9] Herskin J, Steffensen JF. Energy savings in sea bass swimming in a school: measurements of tail beat frequency and oxygen consumption at different swimming speeds. J Fish Biol August 1998;53(2):366–76.
[10] Yang Y, Elgeti J, Gompper G. Cooperation of sperm in two dimensions: synchronization, attraction and aggregation through hydrodynamic interactions. Phys Rev E 2008;78:061903–12.
[11] Olds T. The mathematics of breaking away and chasing in cycling. Eur J Appl Physiol 1998;77:492–7.
[12] Burke E. High-tech cycling. Champaign, Il: Human Kinetics; 1996.
[13] McCole SD, Claney K, Conte JC, Anderson R, Hagberg JM. Energy expenditure during bicycling. J Appl Physiol 1990;68:748–53.
[14] Swain P. Cycling uphill and downhill. Sportscience 1998;2(4). sportsci.org/jour/9804/dps.html Retrieved January 13, 2013.
[15] International Triathlon Union (ITU) Competition Rules part 5.5; January 2011.
[16] Union Cycliste Internationale (UCI) Cycling Regulations, part 2.4.018; January 1, 2013.
[17] McArdle W, Katch F, Katch V. Essentials of exercise physiology, 3rd ed., vol. 1. Baltimore M.D: Lippincott Williams and Wilkins; 2006.
[18] Bogdanis G, Nevill M, Lakomy H, Graham C, Louis G. Effects of active recovery on power output during repeated maximal sprint cycling. Eur J Appl Physiol 1996;74:461–9.
[19] Padilla S, Mujika I, Orbananos J, Santisteban J, Angulo F, Goiriena JJ. Exercise intensity and load during mass-start stage races in professional road-cycling. Med Sci Sports Exerc 2000:796–802.
[20] www.analyticcycling.com.
[21] Trenchard H, Mayer-Kress G. Book of abstracts of international conference on control and synchronization in dynamical systems, held at Leon, Mexico; 2005.
[22] Netlogo User Manual version 5.0.3 October 25, 2012.
[23] Wilensky U. NetLogo flocking model, http://ccl.northwestern.edu/netlogo/models/Flocking, Center for Connected Learning and Computer-Based Modeling, Northwestern University, Evanston, IL; 1998.